

# Seasonally modulated evolutionary dynamics of finite populations: metastable Floquet states

Olena Tkachenko,<sup>1</sup> Juzar Thingna,<sup>2</sup> Sergey Denisov,<sup>1,2</sup> Vasily Zaburdaev,<sup>3</sup> and Peter Hänggi<sup>2</sup>

<sup>1</sup>*Sumy State University, Rimsky-Korsakov Street 2, 40007 Sumy, Ukraine*

<sup>2</sup>*Institut für Physik, Universität Augsburg, Universitätsstraße 1, 86159 Augsburg, Germany*

<sup>3</sup>*Max Planck Institute for the Physics of Complex Systems, Nöthnitzer Str. 38, D-01187 Dresden, Germany*

(Dated: July 29, 2022)

Mating strategies of many biological species are season-dependent. In evolutionary game theory this can be modelled with two finite opposite-sex populations whose members are playing against each other following rules which are modulated in time. By combining Floquet theory and the concept of quasi-stationary distributions, we show the existence of metastable time-periodic states in the stochastic evolution of the populations. These long-lived states describe a fraction of players that are still modifying their strategies and exhibit dynamics beyond the reach of mean-field theory.

PACS numbers: 02.50.Le, 05.45.-a, 87.23.Kg

*Introduction.* The phenotype dynamics in animal populations is tied to the reproductive activity, a complex process which involves mating competitions, courting, and parental care [1]. Within a game theory setup, the sex conflict over parental investment was formalized by Dawkins (1976) in his famous “Battle of Sexes” (BoS) [2]. An example of such a game is shown on Fig. 1. In this game, players of each sex pursue two strategies and the payoff matrix defines the average payoff of a player (which is using a particular strategy) in a round against the whole opposite-sex population. This payoff determines the probability of the player to be selected for reproduction.

In recent years it has been found that in many species mating strategies and preferences are not constant in time but season-dependent [3]. When selecting (courting) a mate, a female (male) of the species faces a complex choice problem where benefits of a choice depend on the season and have to be traded off against each other. For example, the rate of the hormonal activity in the females of Carolina anole lizards (*Anolis carolinensis*), courtship strategies of the males, and mate selection criteria of both, are regulated by the temperature and photoperiod [4]. Even the amount of different types of muscle fibers that control the vibrations of a red throat fan (dewlap) - which males employ during courtship - is season dependent [5]. Within the BoS framework, these seasonal variations can be modeled by periodically modulating the game payoffs as illustrated in Fig. 1. It is the goal of this paper to understand how these modulations influence the game-driven dynamics of populations.

Finite size of animal populations favours a stochastic approach to the problem of evolutionary dynamics. Although the convergence to the deterministic mean-field dynamics is guaranteed in the limit of a large number of players  $N \rightarrow \infty$  [6–8], the stochastic dynamics of large but finite populations can still be very different from the mean-field deterministic evolution [9–12].

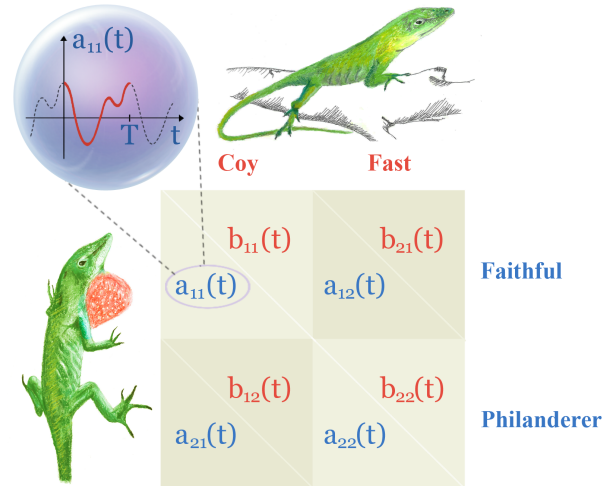


FIG. 1: (color online) ‘Battle of Sexes’ with seasonal variations. A female of Carolina anole lizards could be either *coy* (and prefer a long and arduous courtship, in order to be sure that a mate will contribute to parental care) or *fast* (and not concerned much with the parental care). A male of the species could be either *faithful* (and ready to assure a potential partner that he will be a faithful husband by performing a long courtship) or *philanderer* (and would prefer to shorten the courtship stage). Depending on the strategies,  $s$ , played by the female and  $s'$ , played by her mate, there are payoffs,  $b_{s,s'}$  (to the female) and  $a_{s',s}$  (to the male). Both females and males are season-constrained in their preferences of their mates, which is modelled via time-periodic modulations of the payoffs.

In this Letter, we apply the concept of quasi-stationary distributions in absorbing Markov chains [13] to a stochastic two-player game and identify the *metastable* states. By employing the Floquet theory [14] of matrix operators, used in quantum physics [15], we generalize the notion of metastable states [16, 17] to periodically modulated games. We show that these states survive

over extremely long timescales, as compared to the period of modulations, and demonstrate cyclic polymorphic dynamics which is beyond the reach of the mean-field approach. Floquet metastable states are not only specific to the problem of season-modulated reproduction and can have implications for understanding non-equilibrium dynamics of finite-size systems in general.

*Model.* We adapt the game-oriented version of the Moran processes [18], introduced in Ref. [19] and generalized to two-player games in Ref. [9]. Players  $A$  (males) and  $B$  (females) form two populations, each one of a fixed size  $N$  and with two available strategies,  $s = \{1, 2\}$ , see Fig. 1. Payoffs are specified by four functions,  $\{a_{ss'}(t)\}$  and  $\{b_{s's}(t)\}$ ,  $s, s' = \{1, 2\}$ . They are time-periodic functions,  $c_{ss'}(t) = c_{ss'}(t + T)$ ,  $c = \{a, b\}$ , and can be represented as sums of autonomous and zero-mean non-autonomous components,  $c_{ss'}(t) = \bar{c}_{ss'} + \tilde{c}_{ss'}(t)$ ,  $\langle \tilde{c}_{ss'}(t) \rangle_T = 0$ . The time starting from  $t = 0$  is incremented by  $\Delta t = T/M$  after each round. After  $M$  rounds the payoffs return to their initial values. The state of the populations after the  $m$ -th round is fully specified by the number of players playing the first strategy,  $i$  (males,  $s = 1$ ) and  $j$  (females,  $s' = 1$ ),  $0 \leq i, j \leq N$ . The payoff of the players using strategy  $s$  is

$$\pi_s^A(j, t) = a_{s1}(t) \frac{j}{N} + a_{s2}(t) \frac{(N-j)}{N}, \quad (1)$$

$$\pi_s^B(i, t) = b_{s1}(t) \frac{i}{N} + b_{s2}(t) \frac{(N-i)}{N}. \quad (2)$$

Payoffs determine the probabilities for a player to be chosen for reproduction, e.g. for the male population,

$$P_s^A(i, j, t) = \frac{1}{N} \cdot \frac{1-w + w\pi_s^A(j, t)}{1-w + w\bar{\pi}^A(i, j, t)}, \quad (3)$$

where  $\bar{\pi}^A(i, j, t) = [i\pi_1^A(j, t) + (N-i)\pi_2^A(j, t)]/N$  is the average payoff of the males. The baseline fitness  $w \in [0, 1]$  is a tunable parameter of the game [9, 19]. When  $w = 0$ , the probability to be chosen for reproduction does not depend on player's performance and is uniform across the population. After the choice has been made, another member of the population is chosen completely randomly and replaced with an offspring of the player chosen for reproduction, i.e. with a player using the same strategy as its parent [20]. This update mechanism is acting simultaneously in both populations,  $A$  and  $B$ , such that a mating pair produces two offspring, a male and a female, on every round. The size of the populations is therefore preserved and  $N$  is a game parameter.

A single round can be considered as a one-step Markov process, with transition rates, e.g. for population  $A$ , given by [9, 21]

$$\begin{aligned} T_A^+(i, j, t) &= \frac{1-w + w\pi_1^A(t)}{1-w + w\bar{\pi}^A} \frac{i}{N} \frac{N-i}{N}, \\ T_A^-(i, j, t) &= \frac{1-w + w\pi_2^A(t)}{1-w + w\bar{\pi}^A} \frac{N-i}{N} \frac{i}{N}. \end{aligned} \quad (4)$$

By following the approach in Ref. [9], it can be shown that in the limit  $N \rightarrow \infty$  the dynamics of the variables  $x = i/N$  and  $y = j/N$  is defined by the adjusted replicator equations [7, 22],

$$\dot{x} = [1-x][\Delta^A(t) - \Sigma^A(t)y] \frac{1}{\Gamma + \bar{\pi}^A(x, y, t)}, \quad (5)$$

$$\dot{y} = [1-y][\Delta^B(t) - \Sigma^B(t)x] \frac{1}{\Gamma + \bar{\pi}^B(x, y, t)}, \quad (6)$$

where  $\Delta^C = c_{12} - c_{22}$ ,  $\Sigma^C = c_{11} + c_{22} - c_{12} - c_{21}$ ,  $\Gamma = \frac{1-w}{w}$ , and  $C(c) = \{A(a), B(b)\}$ .

The state of the system can be expressed as a  $N \times N$  matrix  $\mathbf{p}$  with elements  $p(i, j)$ , which are the probabilities to find two populations in the states  $i$  and  $j$ , respectively. Round-to-round dynamics can be evaluated as the multiplication [23] of the state  $\mathbf{p}$  with the transition fourth-order tensor  $\mathbf{S}$ , with elements  $S(i, j, i', j')$  [3]. By using the bijection  $k = (N-1)j + i$ , we can unfold the probability matrix  $p(i, j)$  into the vector  $\tilde{p}(k)$ ,  $k = 0, \dots, N^2$ , and the tensor  $S(i, j, i', j')$  into the matrix  $\tilde{S}(k, l)$ . This reduces the problem to a Markov chain [25],  $\tilde{\mathbf{p}}^{m+1} = \tilde{\mathbf{S}}^m \tilde{\mathbf{p}}^m$ , where  $m$  is the round to be played. The four states ( $i = \{0, N\}, j = \{0, N\}$ ) are absorbing states because the transition rates, Eqs. (4), leading out of them equal zero. The absorbing states are attractors of the evolutionary dynamics, and the finite-size fluctuations will eventually drive a population to one of its absorbing states. This would mean the extinction of all but one phenotype such that only one strategy survives in the now *monomorphic* population [9, 12].

We are interested in the dynamics before the absorption, so we merge the four states into a single absorbing state by summing the corresponding incoming rates. The boundary states, ( $i = \{0, N\}, j \in \{1, \dots, N-1\}$ ) and ( $i \in \{1, \dots, N-1\}, j = \{0, N\}$ ), can also be merged into this absorbing 'super-state': Once the population gets to the boundary, it will only move towards one of the two nearest absorbing states. By labelling the absorbing super-state with index  $k = 0$ , we end up with a stochastic  $(L+1) \times (L+1)$  matrix

$$\tilde{\mathbf{S}}^m = \begin{bmatrix} 1 & \mathbf{g}_0^m \\ \mathbf{0} & \tilde{\mathbf{Q}}^m \end{bmatrix} \quad (7)$$

where  $L = (N-1)^2$ ,  $\mathbf{g}_0^m$  is a vector of the incoming transition probabilities of the absorbing super-state,  $\mathbf{0}$  is a  $L \times 1$  zero vector, and  $\tilde{\mathbf{Q}}^m$  is a  $L \times L$  reduced transition matrix.

With Eq. (7), we arrive at the setup used by Darroch and Seneta to formulate their concept of *quasi-stationary distributions* [13]. There exists a vector  $\tilde{\mathbf{d}}$  with the maximal mean absorption time. This state is the most resistant to the wash-out by the finite-size fluctuations and it remains near invariant under the action of the matrix  $\tilde{\mathbf{S}}^m$ .  $\tilde{\mathbf{d}}$  is the normalized right eigenvector of the reduced transition matrix  $\tilde{\mathbf{Q}}^m$  with the maximum

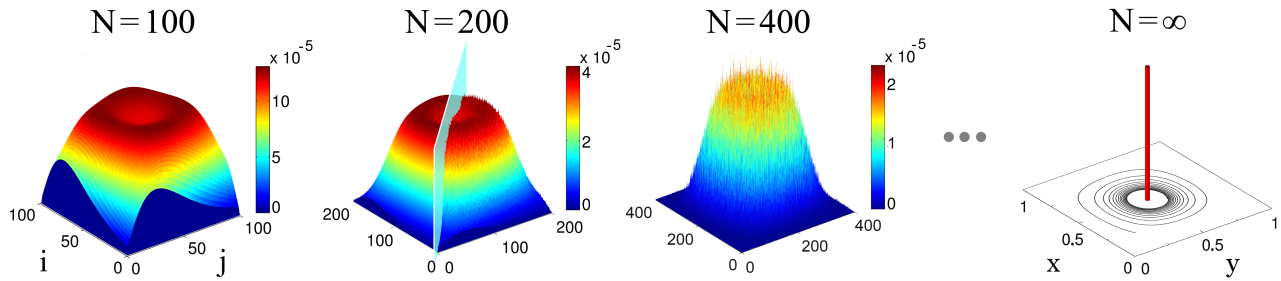


FIG. 2: (color online) Metastable states of the Battle of Sexes with stationary payoffs. In the mean-field limit  $N = \infty$ , a trajectory spirals towards a fixed point attractor  $(\frac{1}{2}, \frac{1}{2})$ , the Nash equilibrium of the game. The metastable states are specified by their quasi-stationary probability density functions (pdf's) (3d plots). With the increase of  $N$ , the functions tend to localize at the Nash equilibrium. Although, for any  $N$ , the mean position  $(\bar{x}(t), \bar{y}(t))$  coincide with the Nash equilibrium, the stochastic evolution is governed by the metastable limit cycles located on the crater ridge on the pdf's tops. For  $N = 200$  the pdf combines the results of the direct diagonalization (left half of the pdf, this procedure was also used to obtain the function for  $N = 100$ ) and of the stochastic sampling (right part of the pdf, this procedure was also used to obtain the function for  $N = 400$ ) [27]. The baseline fitness  $w = 0.3$  (other parameters are given in the text).

eigenvalue  $\lambda$  [24]. By using the inverse bijection, we can transform vector  $\tilde{\mathbf{d}}$  into a two-dimensional probability density function (pdf)  $\mathbf{d}$ .

*Stationary case.* As an example, we consider a game with payoffs  $a_{11}$ ,  $a_{22}$ ,  $b_{12}$  and  $b_{21}$  equal 1, and payoffs  $-1$  for the rest of strategies (this choice corresponds to the ‘‘Matching Pennies’’ game [26]). Figure 2 presents the metastable states of the game. In order to find them we use two methods, the direct diagonalization of the matrix  $\tilde{\mathbf{Q}}$  (the matrix does not change from round to round) and stochastic sampling [27]. The latter was performed by launching trajectories from random initial points, uniformly distributed on the grid  $[1, \dots, N - 1; 1, \dots, N - 1]$  and then updating the histogram with only those which remained unabsorbed after  $10N^2$  rounds. For  $N = 200$  we find a perfect agreement between the results of the two approaches.

The means,

$$\bar{x} = \sum_{i,j=1}^{N-1} \frac{i}{N} \cdot d(i, j); \quad \bar{y} = \sum_{i,j=1}^{N-1} \frac{j}{N} \cdot d(i, j), \quad (8)$$

coincide with the Nash equilibrium [28] for any  $N$ . However, the actual stochastic dynamics is governed by the metastable limit cycle encircling the equilibrium point (this could be seen by performing stochastic simulations and tracking the polar angle), see crater ridges on the tops of pdf's shown in Fig. 2. It can be interpreted as a stochastic Hopf bifurcation [29] within the framework of the stochastic differential equation approach to the dynamics of finite populations [9, 21]. In the mean-field limit, where the noise strength goes to zero, the cycle collapses into the Nash equilibrium. Note that convergence to this limit is slow, as it is indicated by the width of the pdf for  $N = 400$ .

*Case of modulated payoffs.* By adding time-modulations to the model introduced in the previous

section, we find that the mean-field dynamics, Eq. (6), does not exhibit substantial changes even under relatively large modulations. For the choice  $\epsilon(t) = \tilde{a}_{11}(t) = \tilde{b}_{22}(t) = f \cos(\omega t)$  with  $\omega = 2\pi/T$ , and all other payoffs held stationary, there is a period-one limit cycle localized near the Nash equilibrium of the stationary case, see Figs. 3(a,b). It shrinks to a set of adiabatic Nash equilibria,  $\left\{ x_{NE}(\epsilon) = \frac{2-\epsilon}{4-\epsilon}, y_{NE}(\epsilon) = \frac{2}{4+\epsilon} \right\}$  in the limit  $\omega \rightarrow 0$ .

The evolution of a stochastic trajectory, when initiated not too close to the absorbing boundary, can be divided into two consecutive stages. At first the trajectory relaxes towards a metastable attractor. The characteristic relaxation time scales as  $N$ , in accordance with the scaling of time during the transition from a finite- $N$  Markov process to the mean-field dynamics [9]. Then the trajectory wiggles around the attractor until the fluctuations drive it out to the absorbing boundary. Within the rough random-walk approximation, the mean absorption time also scales as  $N$  [30]. However, this estimate neglects the presence of the inner attractive manifold and the fact that the noise strength decreases upon approaching the absorbing boundary. In fact, the absorption time scales as  $N^\alpha$ ,  $\alpha > 1$  [31]. The time window where the metastable state governs the population dynamics is limited by these two times, and the state's relative lifetime thus scales as  $N^\alpha(1 - N^{1-\alpha}) \sim N^\alpha$ , see Fig. 3.

For  $\omega = 0.1$ , the stochastic simulations reveal a metastable attractor in the form of a de-localized period-two limit cycle, different from the period-one limit cycle of the mean-field dynamics, see Fig. 3b. Thus there is a contrast between the evolution of means described by the adjusted replicator equations and the results of the stochastic simulations. This can be resolved by using the concept of quasi-stationary distribution. Namely, the transition matrices, Eq. (7), are round-specific now and form a set  $\{\tilde{\mathbf{S}}^m\}$ ,  $m = 1, \dots, M$  (recall that after

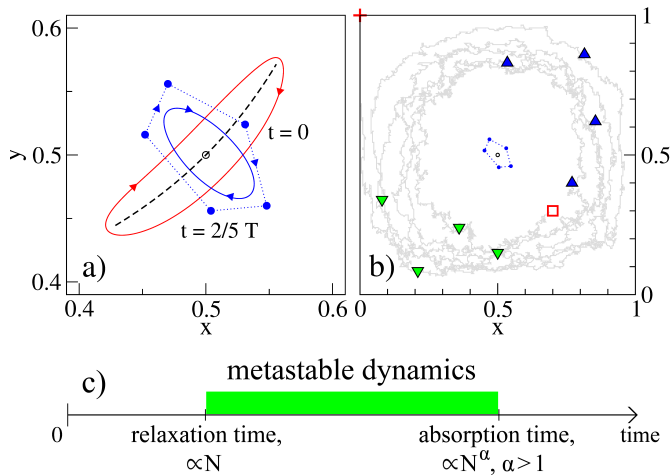


FIG. 3: (color online) Evolutionary dynamics by the Battle of Sexes with modulated payoffs. (a) Period-one limit cycles of the mean-field dynamics,  $N \rightarrow \infty$  with  $\omega = 0.1$  (dash-dotted line) and  $\omega = 0.01$  (solid line), are localized near the point  $(\frac{1}{2}, \frac{1}{2})$  (arrows indicate the direction of the motion). In the limit  $\omega \rightarrow 0$ , the mean-field attractor shrinks to the set of adiabatic Nash equilibria (dashed black line). Mean position of the metastable Floquet state,  $(\bar{x}(t), \bar{y}(t))$ , Eq. (8), moves along the limit cycle localized near the point  $(\frac{1}{2}, \frac{1}{2})$  ( $\bullet$ ; the means are plotted at the instants  $t_n = nT/5$ ,  $n = 0, \dots, 4$ ); (b) A stochastic trajectory (line) reveals the existence of a period-two limit cycle [doubling of the period can be seen from the stroboscopic points, plotted at the instants  $2nT$  ( $\Delta$ ) and  $(2n+1)T$  ( $\diamond$ )]. The trajectory is initiated at the point marked with open square and ends up at the absorbing state (cross at the upper left corner). The parameters are  $f = 0.5$ ,  $N = 200$ , and  $M = T/\Delta t = 10N$  (corresponds to the driving frequency  $\omega = 0.1$  in the mean-field limit) [32]. Other parameters as in Fig. 2; (c) The time window where the metastable dynamics governs the evolution of the system.

$M = T/\Delta t$  rounds the periodically modulated payoffs return to their initial value). The propagator over the interval  $[0, t]$ ,  $0 < t < T$ , is the product  $\tilde{\mathbf{U}}(0, t) = \prod_{m'=1}^{M_t} \tilde{\mathbf{S}}^{m'}$  with  $M_t = t/\Delta t$ . All the propagators, including the period-one propagator  $\tilde{\mathbf{U}}(0, T) = \tilde{\mathbf{U}}_T$ , have the same structure as the supermatrix in Eq. (7). We define the metastable attractor  $\mathbf{d}(T)$  as the quasi-stationary distribution of  $\tilde{\mathbf{U}}_T$ . It is also a *Floquet* state [15] of the reduced propagator  $\tilde{\mathbf{U}}^r(0, T) \equiv \tilde{\mathbf{U}}_T^r$ , which could be obtained by replacing the transition matrices  $\tilde{\mathbf{S}}^{m'}$  with the matrices  $\tilde{\mathbf{Q}}^{m'}$  in the above definition of the propagator (or by simply cutting out the first line and first column from the period-one propagator  $\tilde{\mathbf{U}}_T$ ). It is, therefore, a time-periodic state,  $\mathbf{d}(t+T) = \mathbf{d}(t)$ , which changes during one period of modulations, see Fig. 4a. The metastable state  $\mathbf{d}(t)$  at any instant of time  $t$ ,  $0 < t < T$ , can be found by acting on the state  $\mathbf{d}(0)$  with the reduced propagator  $\tilde{\mathbf{U}}^r(0, t)$ .

The dynamics of the metastable state is consistent with both the mean-field and stochastic results. The evolution

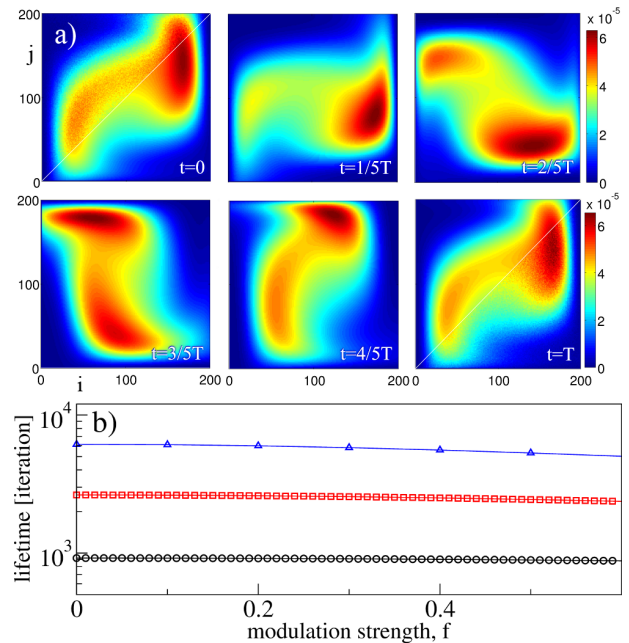


FIG. 4: (color online) (a) Evolution of the metastable Floquet state over one period of modulations. The pdfs obtained by the direct diagonalization of the reduced period-one propagator for  $N = 200$ . The corresponding means  $(\bar{x}(t), \bar{y}(t))$  are shown on Fig. 3a ( $\bullet$ ). Plots for  $t = 0$  (top left part) and  $T$  (bottom right part) also present the results of the stochastic sampling; (b) The lifetime  $t_{\text{life}}$  as a function of the modulation strength  $f$ , for the population size  $N = 50$  ( $\circ$ ),  $100$  ( $\square$ ), and  $200$  ( $\triangle$ ). Other parameters are as in Fig. 2.

of the means,  $(\bar{x}(t), \bar{y}(t))$ , is close to the period-one limit cycle, see blue dots on Fig. 3a, whereas the dynamics of the whole distribution  $\mathbf{d}(t)$ , Fig. 4a, is in agreement with the finite- $N$  dynamics. The Floquet state consists of two opposite peaks produced by the noised period-two limit cycle (compare also the positions of the stroboscopic points in Fig. 3b with the pdf for  $t = 0$  in Fig. 4a). The peak contributions balance each other thus reducing the dynamics of the means to the vicinity of the point  $(\frac{1}{2}, \frac{1}{2})$ .

The lifetime of the state  $\mathbf{d}(t)$  can be characterized with the largest eigenvalue  $\lambda_T$ ,  $0 < \lambda_T < 1$ , of the matrix  $\tilde{\mathbf{U}}_T^r$  [31]. In order to compare it with lifetimes of stationary metastable states, we introduce the mean single-round exponent,  $\bar{\lambda}_T = \lambda_T^{1/M}$  and define the mean lifetime  $t_{\text{life}} = 1/(1 - \bar{\lambda}_T)$ . Figure 4b shows the dependence of  $t_{\text{life}}$  on the strength of modulations. Aside of the slow decay trend, the effect of modulations is not large. This is in stark contrast to the dynamics of the metastable Floquet states. Namely, while in the stationary limit  $\mathbf{d}$  is localized near the Nash equilibrium, at the maximal distance from the absorbing boundaries, the metastable Floquet state in the course of its evolution passes very close to the boundary, see Fig. 4a. The evolution of the polymorphic fraction looks like a repeating sequence of

population bottlenecks [2], yet this only weakly affects the lifetime of the fraction.

*Conclusions.* We presented a concept of metastable Floquet states in game-driven populations when the game payoffs are periodically modulated in time. The idea that Floquet theory could be used to model the evolution of ecological systems subjected to periodic environments, has been recently emphasized in Ref. [33]. It was employed to analyse the stable asymptotic regimes of models described by linear differential equations, in the spirit of the conventional Floquet theory [14]. Here we combined the idea of Floquet states with the concept of quasi-stationary distributions of stationary Markov chains [13]. We are not only motivated by the effects observed by ecologists but also aim at the formulation of a class of states existing in periodically modulated finite systems with stochastic dynamics. Metastable Floquet states may, for example, underlay a gene-expression dynamics in a single-cell, where the chemical kinetics of molecules is modulated by the inner-cell circadian rhythm [34].

S. D. and P. H. acknowledge support by the German Excellence Initiative “Nanosystems Initiative Munich”. J. T. acknowledges the computing time on the GCS Supercomputer SuperMUC at Leibniz Supercomputing Centre.

---

[1] M. Andersson, *Sexual Selection* (Princeton Univ. Press, Princeton, 1994).  
 [2] R. Dawkins, *The Selfish Gene* (Oxford University Press, Oxford, 1976).  
 [3] See Supplementary Material for more information.  
 [4] D. Crews, *Science* **189**, 1059 (1975).  
 [5] M. M. Holmes, C. L. Bartrem, and J. Wade, *Physiol. and Behav.* **91**, 601 (2007).  
 [6] J. Hofbauer, *Imitation dynamics for games* (preprint, 1995).  
 [7] J. Hofbauer and K. H. Schlag, *J. of Evol. Economics* **10**, 523 (2000).  
 [8] K. H. Schlag, *J. of Econom. Theory* **78**, 130.  
 [9] A. Traulsen, J. C. Claussen, and C. Hauert, *Phys. Rev. Lett.* **95**, 238701 (2005).  
 [10] Ch. S. Gokhale and A. Traulsen, *Dyn. Games and Appl.* **4**, 468 (2014).  
 [11] A. Traulsen, J. C. Claussen, and C. Hauert, *Phys. Rev. E* **74**, 011901 (2006).  
 [12] A. Dobrinevski and E. Frey, *Phys. Rev. E* **85**, 051903 (2012).  
 [13] J. N. Darroch and E. Seneta, *J. Appl. Prob.* **2**, 88 (1965).  
 [14] G. Floquet, *Annales de l’École Normale Supérieure* **12**, 47 (1883).  
 [15] M. Grifoni and P. Hänggi, *Phys. Rep.* **304**, 229 (1998).  
 [16] G. Biroli and J. Kurchan, *Phys. Rev. E* **64**, 016101 (2001).  
 [17] S. Rulands, T. Reichenbach, and E. Frey, *J. Stat. Mech.* L01003 (2011).  
 [18] P. A. P. Moran, *The Statistical Processes of Evolutionary*

*Theory* (Clarendon, Oxford, 1962).

[19] M. A. Nowak, A. Sasaki, C. Taylor, and D. Fudenberg, *Nature* **428**, 646 (2004).  
 [20] These two consecutive steps, death and birth, can be reinterpreted as a single step of *imitation*, i.e. adoption of the strategy of the first player by the second one.  
 [21] A. Traulsen, J. C. Claussen, and C. Hauert, *Phys. Rev. E* **85**, 041901 (2012).  
 [22] J. M. Smith, *Evolution and the Theory of Games* (Cambridge University Press, Cambridge, 1982).  
 [23] We follow the “physical” convention that the stochastic matrix acts on the probability vector from the right.  
 [24] By virtue of the Perron-Frobenius theorem,  $\lambda$  and  $\mathbf{d}$  are both real and non-negative [25].  
 [25] E. Seneta, *Non-negative Matrices and Markov Chains* (Springer, NY, 2006).  
 [26] J. von Neumann and O. Morgenstern, *Theory of Games and Economic Behaviour* (Princeton University Press, Princeton, 1944).  
 [27] For  $N = 200$  the diagonalization of the  $39\,601 \times 39\,601$  matrix  $\mathbf{Q}_T$  was performed on the computation cluster of the MIPPKS (Dresden) and Leibniz-Rechenzentrum (München). The stochastic sampling was performed on two GPU clusters (each consisting of six TESLA K20XM cards). That allowed us to obtain  $5 \cdot 10^8$  realizations for each set of parameters.  
 [28] J. Nash, *PNAS* **36**, 48 (1950).  
 [29] L. Arnold, *Random Dynamical Systems* (Springer, NY, 2003).  
 [30] S. Redner, *A Guide to First Passage Processes* (Cambridge University Press, Cambridge, 2001).  
 [31] The average absorption time for a specific initial state,  $t_{abs}(i, j)$ , is defined by the left eigenvector of the reduced propagator  $\mathbf{Q}$  corresponding to the maximum eigenvalue. The mean absorption time can be obtained by averaging  $t_{abs}(i, j)$  over all initial states (different from boundary states), weighted with  $p(i, j)$ .  
 [32] We find a sharp contrast between the mean-field dynamics and the stochastic evolution for this particular choice of  $M$ . For other driving scheme and/or other choice of the game payoffs, the ‘optimal’ value for the period of modulations would be different.  
 [33] C. A. Klausmeier, *Theor. Ecol.* **1**, 153 (2008).  
 [34] S. S. Golden, V. M. Cassone, and A. Li Wang, *Nat. Struct. Mol. Biol.* **14**, 362 (2007); A. Sancar, *Nat. Struct. Mol. Biol.* **15**, 23 (2008).

## SUPPLEMENTARY MATERIAL

### SEASONAL VARIATIONS IN MATE PREFERENCES

Stable time variations were found in the female flycatcher preferences for male forehead patch size that resulted in late-breeding females preferring males with larger patches [1]. It was explained by the fact that in the beginning of the breeding season, large-patched males allocate more resources to courting than to parental care but change their habits to the opposite late in the season. Seasonal variations were also found in fiddle crabs (female

preference to male claw size) [2], two-spotted goby (female preference to overall male size) [3], and sailfin mollies (male preferences for two different kind of females) [4]. There is overall no agreement reached between ecologists on the role the seasonal plasticity in the mate preference (of different sexually selected traits) plays in the determination of the evolution direction of a species, see Ref. [5].

## TRANSITION TENSOR

Here we describe the transition fourth-order tensor  $S^m(i, j, i', j')$  in terms of the rates  $[T_A^{+,-}(i, j, t)$  and  $T_B^{+,-}(i, j, t)]$  for populations  $A$  and  $B$  given by Eq. (4) in the main text. The stochastic Moran process can be expressed as a Markov chain [6]

$$\begin{aligned}
p^{m+1}(i, j) = & [1 - T_A^+(i, j, m\Delta t) - T_A^-(i, j, m\Delta t)] [1 - T_B^+(i, j, m\Delta t) - T_B^-(i, j, m\Delta t)] p^m(i, j) \\
& + T_B^-(i, j + 1, m\Delta t) [1 - T_A^-(i, j + 1, m\Delta t) - T_A^+(i, j + 1, m\Delta t)] p^m(i, j + 1) \\
& + T_B^+(i, j - 1, m\Delta t) [1 - T_A^-(i, j - 1, m\Delta t) - T_A^+(i, j - 1, m\Delta t)] p^m(i, j - 1) \\
& + T_A^-(i + 1, j, m\Delta t) [1 - T_B^-(i + 1, j, m\Delta t) - T_B^+(i + 1, j, m\Delta t)] p^m(i + 1, j) \\
& + T_A^+(i - 1, j, m\Delta t) [1 - T_B^-(i - 1, j, m\Delta t) - T_B^+(i - 1, j, m\Delta t)] p^m(i - 1, j) \\
& + T_A^-(i + 1, j + 1, m\Delta t) T_B^-(i + 1, j + 1, m\Delta t) p^m(i + 1, j + 1) \\
& + T_A^+(i - 1, j + 1, m\Delta t) T_B^-(i - 1, j + 1, m\Delta t) p^m(i - 1, j + 1) \\
& + T_A^-(i + 1, j - 1, m\Delta t) T_B^+(i + 1, j - 1, m\Delta t) p^m(i + 1, j - 1) \\
& + T_A^+(i - 1, j - 1, m\Delta t) T_B^+(i - 1, j - 1, m\Delta t) p^m(i - 1, j - 1).
\end{aligned} \tag{9}$$

The above equation can be recast into

$$p^{m+1}(i, j) = \sum_{i', j'} S^m(i, j, i', j') p^m(i', j'), \tag{10}$$

where the fourth-order tensor  $S^m(i, j, i', j')$  is given by,

$$\begin{aligned}
S^m(i, j, i', j') = & [1 - T_A^+(i', j', m\Delta t) - T_A^-(i', j', m\Delta t)] [1 - T_B^+(i', j', m\Delta t) - T_B^-(i', j', m\Delta t)] \delta_{i', i} \delta_{j', j} \\
& + T_B^-(i', j', m\Delta t) [1 - T_A^-(i', j', m\Delta t) - T_A^+(i', j', m\Delta t)] \delta_{i', i} \delta_{j', j+1} \\
& + T_B^+(i', j', m\Delta t) [1 - T_A^-(i', j', m\Delta t) - T_A^+(i', j', m\Delta t)] \delta_{i', i} \delta_{j', j-1} \\
& + T_A^-(i', j', m\Delta t) [1 - T_B^-(i', j', m\Delta t) - T_B^+(i', j', m\Delta t)] \delta_{i', i+1} \delta_{j', j} \\
& + T_A^+(i', j', m\Delta t) [1 - T_B^-(i', j', m\Delta t) - T_B^+(i', j', m\Delta t)] \delta_{i', i-1} \delta_{j', j} \\
& + T_A^-(i', j', m\Delta t) T_B^-(i', j', m\Delta t) \delta_{i', i+1} \delta_{j', j+1} \\
& + T_A^+(i', j', m\Delta t) T_B^-(i', j', m\Delta t) \delta_{i', i-1} \delta_{j', j+1} \\
& + T_A^-(i', j', m\Delta t) T_B^+(i', j', m\Delta t) \delta_{i', i+1} \delta_{j', j-1} \\
& + T_A^+(i', j', m\Delta t) T_B^+(i', j', m\Delta t) \delta_{i', i-1} \delta_{j', j-1}.
\end{aligned} \tag{11}$$

Above  $i = 0, \dots, N$ ,  $j = 0, \dots, N$ ,  $i' = 0, \dots, N$ , and  $j' = 0, \dots, N$ . Using the bijection explained in the main text, namely,  $k = (N - 1)j + i$  and  $l = (N - 1)j' + i'$  we obtain the required matrix form, see Eq. (7) in the main text.

- 
- [1] A. Qvarnström, T. Pärt, and B. C. Sheldon, *Nature* **405**, 344 (2000).
  - [2] R. N. C. Milner, *et al.*, *Behav. Ecology* **21**, 311(2010).
  - [3] A. A. Borg, E. Forsgren, and T. Amudsen, *Anim. Behav.* **72**, 763 (2006).
  - [4] K. U. Heubel and J. Schlupp, *Behav. Ecol.* **19**, 1080 (2008).
  - [5] V. D. Jennions and M. Petrie, *Biol. Rev. Camb. Philos*

- Soc., **72** (2006).
- [6] A. Trauslen, J.C. Claussen, and C. Hauert, Phys. Rev. E **85**, 041901 (2012).